Trinity University
Digital Commons @ Trinity

Chemistry Faculty Research

Chemistry Department

11-2013

CO Oxidation Over Au/TiO$_2$ Catalyst: Pretreatment Effects, Catalyst Deactivation, and Carbonates Production

Johnny Saavedra
Trinity University, jsaaved1@trinity.edu

Camilah Powell
Trinity University, cpowell1@trinity.edu

Basu Panthi
Trinity University, bpanthi@trinity.edu

Christopher J. Pursell
Trinity University, cpursell@trinity.edu

Bert D. Chandler
Trinity University, bchandle@trinity.edu

Follow this and additional works at: https://digitalcommons.trinity.edu/chem_faculty

Part of the Chemistry Commons

CO oxidation over Au/TiO₂ catalyst: Pretreatment effects, catalyst deactivation, and carbonates production

Johnny Saavedra, Camilah Powell, Basu Panthi, Christopher J. Pursell, Bert D. Chandler *

Department of Chemistry, Trinity University, San Antonio, TX 78212-7200, United States

ABSTRACT

A commercially available Au/TiO₂ catalyst was subjected to a variety of thermal treatments in order to understand how variations in catalyst pretreatment procedures might affect CO oxidation catalysis. Catalytic activity was found to be inversely correlated to the temperature of the pretreatment. Infrared spectroscopy of adsorbed CO experiments, followed by a Temkin analysis of the data, indicated that the thermal treatments caused essentially no changes to the electronics of the Au particles; this, and a series of catalysis control experiments, and previous transmission electron microscopy (TEM) studies ruled out particle growth as a contributing factor to the activity loss. Fourier transform infrared (FTIR) spectroscopy showed that pretreating the catalyst results in water desorption from the surface, but the observable water loss was similar for all the treatments and could not be correlated with catalytic activity. A Michaelis–Menten kinetic treatment indicated that the main reason for deactivation is a loss in the number of active sites with little changes in their intrinsic activity. In situ FTIR experiments during CO oxidation showed extensive buildup of carbonate-like surface species when the pretreated catalysts were contacted with the feed gas. A semi-quantitative infrared spectroscopy method was developed for comparing the amount of carbonates present on each catalyst; results from these experiments showed a strong correlation between the steady-state catalytic activity and amount of surface carbonates generated during the initial moments of catalysis. Further, this experimental protocol was used to show that the carbonates reside on the titania support rather than on the Au, as there was no evidence that they poison Au–CO binding sites. The role of the carbonates in the reaction scheme, their potential role in catalyst deactivation, and the role of surface hydroxyls and water are discussed.

© 2013 Elsevier Inc. All rights reserved.

1. Introduction

CO oxidation over Au-based catalysts has been widely studied because these materials have potential applications in the selective removal of CO from H₂ rich streams (CO Prox) [1–3]. A number of factors appear to contribute to the high activity at low temperatures that these catalyst exhibit, including: the presence of low coordination surface Au atoms, the importance of Au atoms located at or near the metal–support interface, the presence of surface hydroxyls located near the Au, and electronic interactions between the Au nanoparticles and the support [4–9]. Although the reaction stoichiometry is simple, the reaction mechanism for CO oxidation over Au appears to be complex [9,10]. A variety of oxygenated species have also been suggested to play a role in the catalysis, including support hydroxyls [11–15], water [10,16–20], and carbonates [21,22]. Additionally, O₂ activation, which is generally considered to be the key catalytic step, is not well understood [23–26] nor

are the roles of perimeter sites around Au particles [27,28] or the causes of deactivation [29–31].

The catalytic activity reported for CO oxidation over Au catalysts varies widely; as an example, Kung et al. reviewed the reaction rates for CO oxidation using Au/TiO₂ finding up to a 10-fold variation in reaction rates (0.039–0.35 molCO molAu⁻¹ s⁻¹) for catalysts with similar Au particles size (2.1 and 1.7 nm, respectively) [11]. This variance in activity coincides with a lack of agreement regarding activation methods for the catalysts. Specifically, the temperature of calcination used during catalyst preparation varies widely [32–35]. Depending on the synthetic route chosen, activation temperatures range from 200 to more than 400 °C with large differences in the time chosen for activation treatments [36–38].

Bond reviewed the effects of temperature and treatment gas on the preparation of Au catalysts [39]. The main conclusions regarding the activation conditions can be summarized in a few points: (1) Heating in reducing atmospheres (H₂, CO) or Argon at temperatures under 393 K is preferred to oxidizing atmospheres (O₂ or Air) and higher temperatures. This is supported by the fact that reduction to Au⁰ starts at low temperatures and residual Cl⁻ is rapidly eliminated (via HCl). (2) Au particle size increases with

---

increasing treatment temperature, and at temperatures above 573 K, O_2 promotes particle growth more so than H_2 does. (3) Fully reduced particles do not show substantial mobility unless chloride remains on the catalyst surface. Therefore, Bond recommends low temperatures and short treatment times for preparing supported Au catalysts. Bond's considerations regarding the thermal activation are primarily focused on preparing small supported Au nanoparticles in the size regime (2–4 nm) that are catalytically active; however, there is little discussion regarding the effect that these thermal treatments have on the resulting catalytic activity.

The literature provides a wide variety of activation protocols (both oxidative and reductive) for Au-based catalysts [11,46]. Table 1 summarizes several different activation protocols applied to Au/TiO$_2$ catalysts and includes the size of the Au particles produced and the reported catalytic activities (CO oxidation between 273 and 300 K). It is readily apparent that there is almost no correlation between the pretreatment temperatures used and the catalytic activity reported. Catalysts with very similar Au particle sizes may differ by an order of magnitude. This may be influenced by residual chloride in the less active catalysts, as chloride is well known to be a poison for CO oxidation over Au catalysts [47]. Additionally, several studies report catalytic activities of approximately 0.1–0.3, yet the pretreatments differ by 300 K and up to 12 h. Given this variance in the literature, one might posit that pretreatment protocols are relatively unimportant so long as relatively small particles are maintained and chloride is sufficiently removed.

Behm et al. more systematically varied activation protocols to produce more active Au–CO oxidation catalysts [30]. They found that annealing the catalyst with a mixture H_2/N_2 at 473 K was more effective than the conventional oxidation at 673 K. They also pointed out that more severe reductions (with H_2/N_2 mixtures at 673 K) produce catalysts with a higher tendency for deactivation [30].

In preliminary studies using a commercial Au/TiO$_2$ sample, we found that changes in pretreatment conditions immediately prior to catalytic testing produced similarly marked variations in catalytic activity. We therefore undertook a more detailed examination of how thermal treatments change the catalyst in order to better understand the factors that control CO oxidation activity. Seven thermal treatments were chosen to prepare catalysts with markedly different reaction rates. These induced differences in catalytic activity were the basis of an experimental design composed of three related studies. First, the CO adsorption thermodynamics were studied to evaluate electronic changes to the Au nanoparticles. Second, a Michaelis–Menten analysis of CO oxidation kinetics measurements was used to evaluate changes in O_2 reactivity and in the relative number of active sites. Finally, in situ IR spectroscopy was used to monitor changes in surface composition caused by

thermal treatments and during CO oxidation catalysis. These experiments provide a more complete picture of how the catalyst changes (and does not change) as a function of thermal treatments.

2. Experimental

2.1. Materials

The catalyst used in this study was a commercial AUROlite™ sample purchased from STREM Chemicals (nominal 1% Au/TiO$_2$). This catalyst was pretreated by the manufacturer to ensure that particles were of appropriate size (2–4 nm) to yield active CO oxidation catalysts. Further, this catalyst has proven to be active and stable over long periods of time [48,49]. The catalyst was crushed and stored in a dark refrigerator. Gases (N_2, H_2, O_2, and 5%CO/He) were 5.0 grade supplied by Praxair and used with no additional purification. Powdered Silicon Carbide (400 mesh) was purchased from Aldrich.

2.2. Catalyst pretreatments

Catalyst pretreatment was performed in situ at atmospheric pressure using various gas mixtures at 100 mL/min; heating rates were 5 °C/min. Treatment conditions are detailed in Table 2. After each treatment, the catalyst was purged with N_2 for 60 min at the treatment temperature and subsequently cooled to ambient temperature.

2.3. CO oxidation catalysis

The CO oxidation reactor consisted of a home-built laboratory-scale single-pass plug-flow micro-reactor [48,49]. The reaction zone consisted of 5 mg of finely ground fresh catalyst diluted in 750 mg of silicon carbide. Gas flows were controlled with 4 electronic low pressure mass flow controllers (Porter Instruments). The composition of the feed and reactor effluent (CO and CO_2) was determined using a Siemens Ultramat 23 IR gas analyzer.

Each treatment-reaction sequence was performed with a fresh sample of catalyst. After loading into a glass U-tube, the diluted catalyst was treated with one of the procedures shown in Table 2. CO oxidation activity was measured in a 60-min experiment immediately following the pretreatment. The feed (1% CO, 20% O_2, balance N_2, flowing at 180 mL/min; $WHSV = 2.16 \times 10^3 \, L \cdot h^{-1} \cdot g_{cat}^{-1}$) was held constant and the reaction temperature was maintained at 20 °C using a water bath.

O_2 pressure dependence was determined in separate experiments. After treating 4 mg of catalyst and cooling under N_2, the reactor was fed with 140 mL/min of a gas mixture containing 1%

Table 1
Activation conditions, Au particle size, and catalytic activity of Au/TiO$_2$ catalysts used in low-temperature CO oxidation (273–300 K).

Activation conditions	Au particle size (nm)	Rate/Au$_{tot}$ (s^{-1})	T (K)	Ref.
No thermal treatment	2.9 ± 1.7	0.03	298	[7]
298 K, 1 h, H_2	2	1.4 ± 0.2[a]	273	[40]
310 K, 24 h, air	3.3 ± 0.5	0.34[b]	273	[41]
373 K, 1 h, H_2 + 298 K, CO/O_2	1.7	0.35	273	[23]
373 K, 0.5 h, H_2 + 373 K, 0.5 h H_2O/H_2	3.3 ± 0.7	0.013[b]	288	[10]
523 K, 0.5 h, air	3	3.0[b]	298	[20]
573 K, air	2.1	0.025	298	[42]
623 K, 4 h, He	3.3 ± 0.5	0.18[b]	298	[43]
623 K, 4 h, air + vacuum dried	3.0 ± 1.3	0.16	273	[8]
673 K, 4 h, air + 723 K, 10 h H_2	2.9 ± 0.5	0.13	300	[44]
673 K, 1 h 1% CO, 21% CO in Ar	2.1	0.039	273	[45]

[a] Based on the reaction of adsorbed CO species.
[b] Based on surface Au.

Table 2
Catalyst pretreatment conditions.

Pretreatment	Gas mix[a,b]	Temperature (°C)[c]	Time (h)
None	No gas flow	–	0
O_2-A	20% O_2	150	1
H_2-A	20% H_2	150	1
H_2 and O_2	10% O_2 + 10% H_2	250	1
O_2-B	20% O_2	250	16
H_2-B	20% H_2	250	16
O_2-C	20% O_2	350	16

[a] All gases were balanced with N_2 to 100 mL/min.
[b] After every treatment, the sample was purged with N_2 for 1 h at the treatment temperature.
[c] Heating rate was 5 °C/min for all pretreatments.

CO and variable fractions of O_2 (25%, 20%, 15%, 10% and 5%; WHSV = 2.10×10^3 L · h^{-1} · g$_{cat}^{-1}$). After equilibrating the gas flow for 6 min, the catalytic activity was measured and the O_2 flow was changed to the next set-point, maintaining a total flow of 140 mL/min with N_2. The catalytic activity was corrected for any deactivation assuming a linear decrease in activity over time according to a previously described methodology [48].

2.4. CO heat of adsorption measurements via IR spectroscopy

Catalyst samples (30 mg) for CO adsorption experiments were treated using the 7 pretreatments described in Table 2. The treatment setup was similar to the CO oxidation reactor and consisted of a fritted U-tube quartz reactor located in a Thermolyne furnace; heating rates were 5° C/min. The gas mixture was prepared in an external manifold using low pressure rotameters. After treatment, the samples were flushed with N_2 for 1 h at the treatment temperature, cooled to room temperature, and stored in a dessicator in a closed, foil-wrapped vial until IR measurements (typically 12–16 h).

CO adsorption experiments were performed as previously described [50,51]. Briefly, approximately 25 mg of a pretreated sample was pressed into a 30×30 Ti mesh (Unique Wire Weaving Co.). The mesh-supported pellet was mounted into a custom-built copper cell and vacuum chamber (International Cryogenics) with a gas-phase optical path length of 1.2 cm. The vacuum chamber was placed in the sample compartment of a Nicolet Magna 550 FTIR spectrometer and evacuated to a pressure of <1 mTorr for 30–60 min. All measurements were made at ambient temperature and all spectra were referenced to a background spectrum of the catalyst pellet under vacuum prior to the addition of CO. Transmission spectra consisted of 100 scans collected with 8 cm^{-1} resolution (spectral data spacing = 4 cm^{-1}) and were reported in absorbance units.

The gas-handling system consisted of a mechanical pump and liquid nitrogen trap, a glass line with stainless steel transfer lines to the sample apparatus, and a Baratron pressure gauge (P = 0–20 Torr). A liquid nitrogen trap was used to trap out any impurities from the CO tank (UHP Grade, from Air Products). The entire gas-handling system was rinsed with CO three times before exposing the sample. After collecting a background spectrum, the sample was exposed to a low pressure of CO and the surface was allowed to equilibrate for 5–10 min; previous work has shown that this is ample time for CO equilibration on Au catalysts [48,50,51]. An infrared spectrum was recorded and the pressure in the cell was slowly increased to the next pressure. After completing an experiment, the sample was evacuated and the experiment repeated for a total of two or three adsorption isotherm measurements on a single catalyst sample in a single day.

2.5. In situ FTIR measurements

A previously described home-built flow IR cell was used for the in situ FTIR experiments [52–55]. The cell consisted of a stainless steel chamber wrapped by a heating mantle (up to 400 °C) with two IR transparent KBr windows. Gases were mixed in an external stainless steel manifold using low-pressure rotameters. The gas cell was fed with 100 mL/min of gas mixtures and heated at a constant rate of 5 °C/min.

The catalyst (35 mg) was finely ground in an agate mortar, pressed into a 13 mm circular pellet using a stainless steel die and a manual hydraulic press (5 metric tons of pressure for 2 min). The pellet was mounted into the cell and placed in the sample compartment of a Nicolet FTIR spectrometer where a thermocouple adjacent to the pellet monitored the temperature.

Prior to any treatment, a background spectrum of the catalyst pellet in the sample cell was collected. The catalyst pretreatment was carried out in situ using 100 mL/min of the gas mixture at different temperatures (150, 250, and 350 °C; WHSV = 2.00×10^2 L · h^{-1} · g$_{cat}^{-1}$). After treatment, the sample was purged for 1 h and cooled to room temperature under N_2 flow. Spectra were collected at 20 °C and the temperature was kept constant using a coil with recirculating water.

Immediately after treatment, the sample was cooled and a reference spectrum was collected once the temperature was equilibrated at 20 °C. The catalyst pellet was then used for the in situ CO oxidation reaction. The CO oxidation reaction consisted of 4 steps: (a) 10 min flowing with a 1% CO mixture, (b) 10 min with our standard CO oxidation mixture (1% CO, 20% O_2), (c) 10 min flowing with a 1% CO/He mixture, and (d) 10 min purging with N_2. Spectra were collected every 2.5 min.

3. Results

CO oxidation over supported Au catalysts, particularly Au/TiO$_2$, has been widely studied [1–3]. However, substantial differences in CO oxidation activity have been reported, and there is no clear consensus on the best method to achieve maximum catalytic activity and/or to reduce the pronounced deactivation to which these catalysts are prone. We therefore set out to perform a systematic study of pretreatment conditions on CO oxidation catalysis with the goal of understanding how temperature and pretreatment gas composition influence catalytic activity.

3.1. CO oxidation activity

This catalyst has been previously examined with TEM and the average Au particle size was determined to be 3.2 nm, corresponding to a dispersion of 35–40% [49]. Further, controlled poisoning experiments suggested that 11% of the total Au (25–30% of the surface Au) was active in the reaction [48]. This corresponded well with the expected total number of corner and edge atoms in the sample [48]. CO oxidation activity is reported as a catalyzed reaction rate (v, moles of CO converted per total mole of Au in the sample per second); the results are presented in Fig. 1. For all the pretreatments, there is a substantial deactivation over the first 5–10 min on stream. After 20 min of reaction, a quasi-steady state is reached, and the deactivation rate is similar for all the samples.

The catalytic activity in this quasi-steady state is related to the conditions used during the pretreatment step. The untreated catalyst is both active and stable; the use of thermal treatments in the presence of H_2 or O_2 reduces the catalytic activity significantly. Further, as the treatment temperature is increased, catalytic activity becomes progressively lower. As an example, O_2 treatments at 150, 250 and 350 °C (treatments O_2-A, O_2-B and O_2-C, respectively)
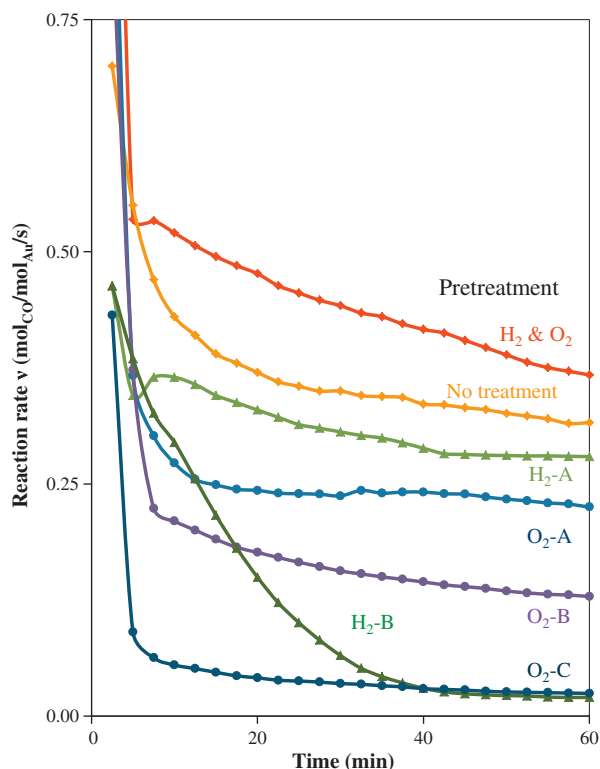
Fig. 1. CO oxidation catalytic activity at 20 °C after various pretreatments. Reaction conditions: 180 mL/min of a 1% CO and 20% O_2 feed; WHSV = 2.16×10^3 L · h^{-1} · g$_{cat}^{-1}$.

reduce the activity by 33%, 50%, and 81%, respectively compared to the untreated catalyst. Similarly, activity drops by a factor of 10 (relative to no pretreatment) when the catalyst is treated at 250 °C under H_2 (treatment H_2-B), although the deactivation that occurs when the catalyst first comes in contact with the feed is markedly slower for this pretreatment. The treatment with a combination of H_2 and O_2 was the only pretreatment that increased the catalytic activity, enhancing it by about 25% relative to no pretreatment.

The remainder of the work in this study was performed to understand why the various pretreatments resulted in catalysts with such markedly different activities. The first possibility we considered was sintering. Given the relatively low treatment temperatures and the drastic changes in activity, this is unlikely. Our previous TEM studies on this catalyst have shown that this catalyst can be treated at 300 °C for 16 h with no changes in the observed particle size [49]. This is a more forcing treatment than all but one of the treatments employed in the present study. Further, careful examination of the first 10 min on stream (Fig. 1) shows that all of the catalysts are initially quite active; the lower steady-state rates are due to deactivation when the catalyst comes in contact with the feed.

To eliminate sintering as a contributing factor to the observed loss of activity, we performed two additional control experiments: (1) A fresh sample was treated with the O_2-C protocol (350 °C, 16 h) followed by the $H_2 + O_2$ treatment (250 °C, 1 h) and (2) a fresh sample was treated with the H_2-B protocol (250 °C, 16 h) followed by the $H_2 + O_2$ treatment (250 °C, 1 h). In both of these experiments, the steady-state catalytic activity (20 min TOS) was essentially the same (within 6%) as the untreated catalyst, i.e., substantially higher than the steady-state activity for the O_2-C or H_2-B treatment alone. The high activity found when the $H_2 + O_2$ treatment is performed after the "deactivating" treatments therefore

excludes nanoparticle sintering as a cause for the deactivation and shows that the deleterious effects that the forcing pretreatments induce are at least partially reversible.

3.2. Infrared spectroscopy of CO adsorption

Infrared spectroscopy can be used to quantify CO adsorption on Au catalysts and extract thermodynamic metrics for CO binding [48,50,51]; in this case, we used the CO adsorption metric to evaluate potential changes to the Au particles. Details of the data collection and analysis can be found in separate publications [48,50,51]. Briefly, the peak area assigned to CO adsorbed on Au is used to determine an adsorption isotherm which is fit to a Temkin adsorption model [48,50,51].

The linear portion of the data (usually corresponding to surface coverages between θ = 0.2–0.8) and a previously determined ΔS_{ads} value of -140 J/mol K were used to extract two descriptive values for each catalyst [50]. The heat of adsorption at zero coverage (ΔH_0), which is determined from the y-intercept of the linear data, describes the nascent binding energy for CO on the catalyst when no adsorbate–substrate interactions are present. The second value, $\delta \Delta H$, describes the change in the adsorption energy from θ = 0 to θ = 1 (i.e., ΔH_0 to ΔH_1). In this case, full coverage represents saturation of the CO binding sites, which is a subset of the total number of surface Au sites. According to the Temkin adsorbate interaction model, this change is attributed to electronic interactions between the CO adsorbates and the Au nanoparticles and thus describes how the surface electronics change with coverage [50,51].

Representative CO adsorption data for each of the various pretreatments are shown in Fig. 2; extracted values for ΔH_0 and $\delta \Delta H$ are shown in Table 3. All of the extracted ΔH_0 and $\delta \Delta H$ values were essentially the same regardless of the pretreatment, indicating that the pretreatments had essentially no effect on the Au–CO interactions [56]. As discussed above, since the adsorption metrics have a particle-size dependence, this result is consistent with a lack of change in particle size with the pretreatments [57]. Our previous NaBr poisoning study showed that $\delta \Delta H$ values can be very sensitive to adsorbates even at low coverages [48]; however, there are essentially no changes observed for the different pretreatments. The key result here is that the CO adsorption metrics indicate that the various pretreatments cause little to no changes in the
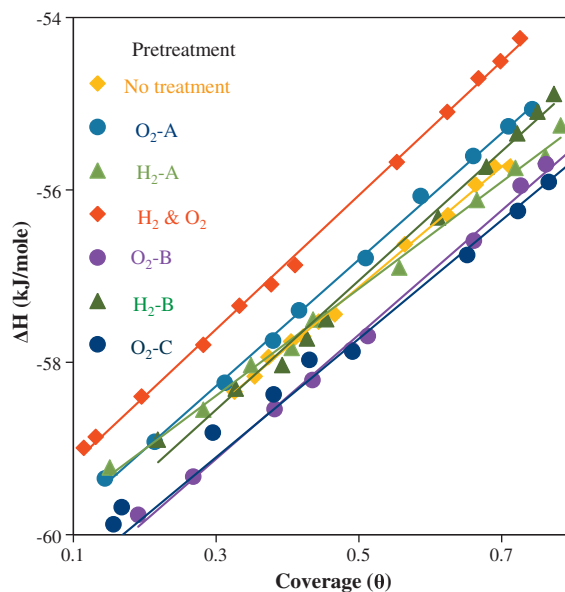

Fig. 2. CO adsorption data ΔH vs. coverage for the various catalyst pretreatments.

Table 3
Thermodynamic metrics for CO adsorption after different activation procedures. Data show averages and standard deviations for 3 measurements on each catalyst.

Pretreatment	$-\Delta H_0$ (kJ/mol)	$-\delta\Delta H$ (kJ/mol)
None	61.4 ± 0.4	7.2 ± 0.5
O_2-A	61.3 ± 0.4	7.9 ± 0.7
H_2-A	61.3 ± 0.4	7.9 ± 0.7
H_2 and O_2	61.9 ± 0.8	7.8 ± 0.1
O_2-B	62.1 ± 0.5	8.0 ± 0.7
H_2-B	60.9 ± 0.3	6.8 ± 0.7
O_2-C	62.1 ± 0.5	8.0 ± 0.7

fundamental Au–CO interactions, indicating that the pretreatments induce no substantial electronic changes to the Au.

3.3. Effect of pretreatments on catalyst surface

Pressed catalyst pellets were placed in an in situ IR spectroscopy cell and treated with the different procedures shown in Table 2. Changes to the catalyst were monitored using IR spectroscopy by collecting spectra after the catalyst returned to ambient temperature. A spectrum of the fresh (untreated) catalyst was collected prior to the pretreatment and used as the background. The resulting spectra are shown in Fig. 3. Because these
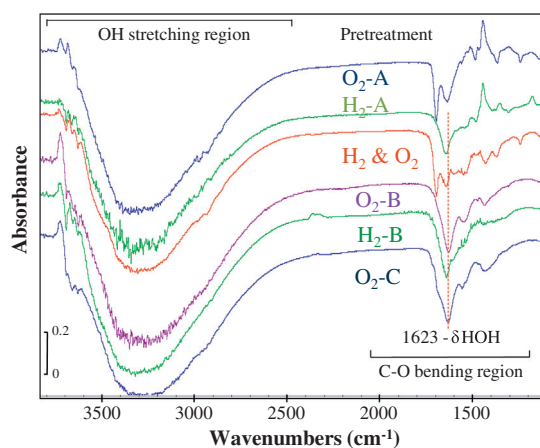

Fig. 3. FTIR spectra of the catalyst after different treatments. Spectra were collected at 20 °C and referenced to fresh untreated catalyst.

are difference spectra, a loss of absorbance indicates a loss of a surface species associated with that particular vibration.

All of the spectra show that absorbance decreases in the broad OH stretching region (3800–2500 cm^{-1}) and at 1623 cm^{-1}, which is attributed to the δ_{HOH} vibration of adsorbed water [58]. These changes are attributed to the loss of adsorbed water and surface hydroxyl groups on the support. Some of the spectra show small changes in the 1800–1200 cm^{-1} region that may correspond to small amounts of surface carbonates. However, there are no consistent changes in this region, or in the entire spectral range for that matter, that can be associated with a systematic change in the catalysts upon the heating under H_2 and/or O_2. In spite of the differences in treatment temperature, the magnitudes of the observed changes to the catalysts are all very similar. There are no obvious differences in the degree of surface hydroxylation that might be correlated with the drastic changes in activity. That is, the higher temperature pretreatments did not cause substantially greater observable surface dehydroxylation or dehydration than did the lower temperature treatments.

3.4. CO oxidation kinetics metrics

Since the pretreatments appeared to induce few if any changes to the Au particles, we next consider potential changes to the catalytic active site using a Michelis–Menten (M–M) kinetic treatment that we have previously developed and employed [48,49,59]. In this treatment, activity data as a function of oxygen pressure can be evaluated with double reciprocal plots (Fig. 4) to provide a means of extracting quantitative parameters that describe O_2 reactivity for individual gold catalysts. A full derivation of this treatment has been previously published [49]. Briefly, a simple characterization mechanism (Scheme 1), which has also been suggested by DFT calculations [3], is used to describe the reaction. We note that this is an intentionally simplified characterization mechanism that may not capture all of the molecular complexity of every elementary step in the reaction mechanism. Further, the mechanism is intentionally vague regarding the nature of the O_2 binding site – the purpose is to evaluate changes to the number of active sites rather than to presuppose the structural characteristics of the O_2 binding site. Hence, the only structural requirement is that oxygen binding occurs in close proximity to Au–CO sites.
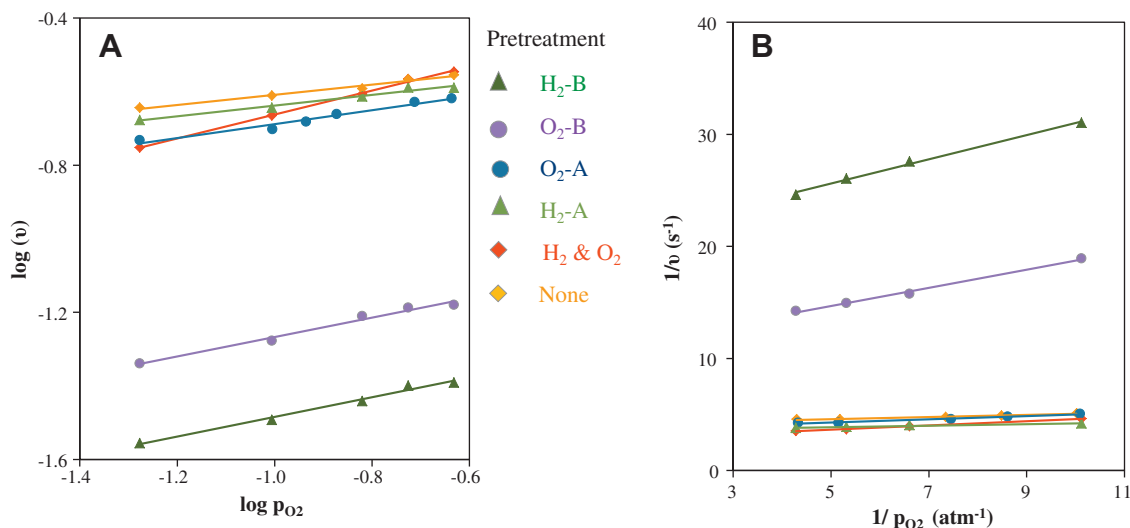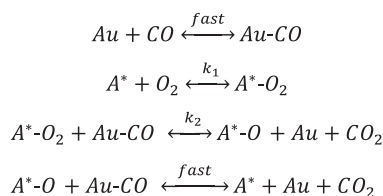

Fig. 4. Kinetic plots for CO oxidation at 20 °C after the various pretreatments. (A) Oxygen reaction order and (B) double inverse plot used in Michaelis–Menten kinetic data treatment (Eq. (1)). Data were corrected for any deactivation assuming a linear loss of activity with time during quasi-steady-state conditions (see Ref. [39]).

$$Au + CO \xleftrightarrow{fast} Au\text{-}CO$$

$$A^* + O_2 \xleftrightarrow{k_1} A^*\text{-}O_2$$

$$A^*\text{-}O_2 + Au\text{-}CO \xleftrightarrow{k_2} A^*\text{-}O + Au + CO_2$$

$$A^*\text{-}O + Au\text{-}CO \xleftrightarrow{fast} A^* + Au + CO_2$$

Scheme 1. Characterization mechanism for the Michaelis–Menten kinetic treatment of CO oxidation catalysis.

In the development of this method, adsorption of CO and activation of O_2 are considered the key kinetic steps; desorption of produced CO_2 and regeneration of the active site are considered to be fast and after the rate determining steps and are therefore kinetically unobservable. Applying a typical kinetic derivation employing the steady-state approximation yields the following expression:

$$\frac{1}{v_{rxn}} = \frac{K_R}{v_{max}}\left(\frac{1}{P_{O_2}}\right) + \frac{1}{v_{max}} \tag{1}$$

where v_{rxn} is the measured reaction rate and

$$v_{max} = k_2\theta_{CO}[A^*]_T \tag{2}$$

and

$$K_R = \frac{k_{-1} + k_2\theta_{CO}}{k_1} \tag{3}$$

We note that a similar set of equations can be derived using a Langmuir–Hinschelwood mechanism, although this requires additional assumptions [49]. In these equations, θ_{CO} designates the coverage of the CO binding sites, which are a subset of the total Au surface sites, and $[A^*]_T$ is the total number of active sites. The total number of active sites is also assumed to involve a subset of the total number of surface Au sites. K_R and v_{max} are descriptive kinetic parameters comparable to those employed in enzyme kinetics [60]. Analogous to the Michaelis–Menten constant, K_R is a measure of the reactivity or instability of adsorbed O_2 (cf. A^*–O_2). Similarly, v_{max} depends both on the intrinsic reaction barrier and the number of active sites. This kinetic treatment has been previously published and has been shown to well describe kinetic data for CO oxidation over several Au [48,49] and bimetallic NiAu [59] catalysts, including a series of intentionally poisoned Au catalysts [48].

One of the primary utilities of the M–M kinetic treatment is that it provides measures of both the intrinsic activity of the active sites (K_R) and the total number of active sites (proportional to v_{max}). Applying this kinetic model to the thermal pretreatments used in this study can therefore help distinguish between changes in the number of active sites and the inherent reactivity of the active sites. The data in Table 4, which is extracted from the data in Figs. 1 and 4, show that K_R is relatively unaffected by the catalyst pretreat-

ment; there are only fluctuations in the K_R values and there is no trend correlating the K_R values with the pretreatments. This indicates that the intrinsic activity of the active sites is relatively unchanged by the pretreatment—even for those catalysts that show severe deactivation. The v_{max} values, on the other hand, change significantly according to the treatment procedure used in activation. The most forcing conditions (temperatures $\geqslant 250$ °C) yield a catalyst with very small values of v_{max}, which is an indication that fewer O_2 activation sites remain active under the quasi-steady-state conditions, i.e., the pretreatments result in a loss of steady-state active sites. Less variation in v_{max} is observed for the mild (250 °C) treatments, which is consistent with their activities being close to that of the untreated catalyst. The v_{max} values are extrapolated values (to infinite oxygen pressure), so they have inherently larger errors associated with the data range employed. In this case, we are only able to differentiate between catalysts that have substantially different numbers of active sites.

3.5. IR spectroscopy during CO oxidation

In situ IR spectroscopy was used to evaluate changes to the catalyst surface under the CO oxidation gas feed. Immediately after the pretreatment and extensive flushing with N_2 (1 h at 20 °C), the catalyst was exposed to the same CO + O_2 gas mixture used for the activity study shown in Fig. 1. This resulted in substantial changes to the IR spectrum of the catalyst. Fig. 5 shows examples of the fresh (untreated) catalyst and the catalyst treated with the procedure H_2-B after 10 min under CO oxidation conditions. The double peak in the range of 2200–2000 cm^{-1} was assigned to gas-phase CO; this peak is accompanied by a single narrow peak at $\sim$2100 cm^{-1} consistent with CO adsorbed on Au (Au–CO) [61,62]. The peaks in the 2400–2300 cm^{-1} are assigned to gas-phase CO_2 resulting from the catalysis. The most substantial changes are the multiple peaks at lower wavenumbers (1800–1200 cm^{-1}). These peaks appear essentially immediately upon introducing the reactant feed to the catalyst and are assigned to carbonate species on the catalyst surface [31,36,63]. The buildup of carbonates on Au/TiO_2 catalysts during CO oxidation has been previously reported in the literature [29,31], and bands at 1537
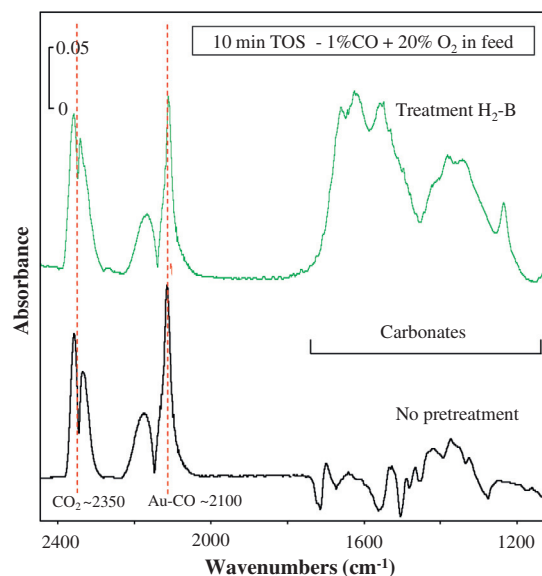
Table 4
Kinetic data for CO oxidation at 20 °C. Quasi-steady-state catalytic reaction rate (v), O_2 reaction order, K_R, and v_{max} values calculated using plots from Fig. 4 and Eq. (1).[a]

Pretreatment	v^a (s^{-1})	O_2 order	K_R (atm^{-1})	v_{max} (s^{-1})
None	0.36	0.13	0.028	0.29
H_2-A	0.33	0.24	0.046	0.29
O_2-A	0.24	0.18	0.047	0.28
H_2 and O_2	0.45	0.32	0.048	0.33
O_2-B	0.18	0.26	0.036	0.08
H_2-B	0.15	0.26	0.038	0.05
O_2-C[b]	0.07	–	–	–

[a] Reaction rate extracted from Fig. 1 at 20 min TOS.
[b] Treatment O_2-C resulted in catalytic activity that was too low to perform an oxygen dependence study.

Fig. 5. IR spectra during CO oxidation (10 min TOS) for the untreated and H_2-B treated catalyst. Gas-phase CO_2 (two bands centered at 2350 cm^{-1}), gas-phase CO (2 bands centered at 2150 cm^{-1}), Au–CO (narrow peak at $\sim$2100 cm^{-1}), and carbonates region (several peaks in the 1800–1200 cm^{-1} region).

and 1357 cm^{-1} have been previously attributed to carbonates formed on TiO$_2$ [30].

There are clear differences in the sizes of the carbonate peaks. The H$_2$-B treated catalyst, which is essentially inactive, has very large carbonate peaks while the more active untreated catalyst has relatively few. Under the conditions of our IR experiment, carbonate production occurs immediately upon contact with the CO + O$_2$ feed; catalyst spectra generally did not change significantly after 5 min TOS. This is largely consistent with the rapid deactivation observed in Fig. 1. Further, the differences in surface carbonates production are the first substantial differences between pretreatments that we have observed; combined with the rough correlation between rapid carbonates buildup and rapid deactivation, this suggest that carbonates may be responsible for the differences in catalytic activity. However, it is unclear if the carbonates reside on the support, on the gold, or on both the Au and the support. Additionally, although IR peak areas are generally proportional to surface concentrations in transmission experiments, it is difficult to compare these peaks from one catalyst pellet to another. There are simply too many variances in local pellet thickness where the IR beam passes to reliably make quantitative comparisons based on the carbonates peak areas alone.

3.6. Effect of carbonates on catalytic activity

To address these questions, we designed a sequential IR experiment that allows us to (i) quantify the carbonates buildup, (ii) compare carbonates buildup between catalysts, and (iii) assess whether the carbonates poison Au surface sites. This procedure is outlined in Scheme 2. After pretreatment and flushing with N$_2$, the catalyst was first contacted with a CO feed (no O$_2$) to measure the area of the Au–CO peak ($\bar{v} \sim 2100$ cm^{-1}; step a). This peak area acts as an internal standard to which subsequent peaks can be compared. The catalyst was then placed under CO oxidation conditions for 10 min (step b), which is sufficient time to allow the carbonates to build up, *vide supra*. The catalyst is then flushed with CO again (step c) to measure changes to the Au–CO peak area and thus evaluate whether the carbonates directly poison the Au sites. Finally, the catalyst was flushed with N$_2$ (step d) to evaluate relative amounts of strongly and loosely bound carbonates.

IR spectra in the 1800–1200 cm^{-1} region (collected after step b) for the various pretreatments are shown in Fig. 6. The peaks in Fig. 6 are all broad and do not warrant individual assignments (e.g., carbonate, bicarbonate, monodentate, or bidentate on Au or TiO$_2$); therefore, all the IR signals between 1800 and 1200 cm^{-1} were considered carbonate-like species formed during CO oxida-tion. To quantify their production, the entire 1800 and 1200 cm^{-1} region was integrated as a whole; no individual assignments were made.

The peak areas measured from the spectra in Fig. 6 were normalized to the area of the peak assigned to Au–CO collected in step a of Scheme 2. The CO heat of adsorption experiments (*vide supra*) justify this methodology as they showed no change in Au–CO interactions as a function of pretreatment. Further, the Au–CO peak area data (Table 5) are similar for all the pretreatments and show only random variation associated with reasonable experimental uncertainty in the catalyst pellet mass and local thickness in areas through which the IR beam passed [64].

Fig. 7 plots the quasi-steady-state catalytic activity (Fig. 1, Table 4) vs. the normalized carbonates peak area. These data show an excellent correlation between the catalytic activity and normalized carbonates area. Two areas for the carbonates peaks were measured for each pretreatment: one immediately after CO oxidation was finished (end of step b in Scheme 2) and a second after the catalyst had been flushed to remove any weakly adsorbed carbonates. There was generally very little change in the carbonates area upon flushing, indicating that they are strongly bound to the catalyst surface.

Fig. 7 shows a clear correlation between catalytic activity and the amount of surface carbonates produced in the reaction. Further, the degree to which the surface carbonates are deposited is determined by the pretreatment used during catalyst activation. Harsh treatments (longer times and/or higher temperatures) yield catalysts that accumulate large quantities of carbonates and have low activities; mild treatments yield more active catalysts that have relatively few carbonates on the surface.

3.7. Effect of carbonates on CO adsorption

The kinetics studies (Table 4) indicate that the inherent reactivity of the active sites (described by K_R) remains essentially the same for all the pretreatments; the reduced catalytic activity (nominally quantified by changes in v_{max}) appears to be due to a loss of active sites. It is possible that this is associated with carbonates depositing on the Au particles, thus preventing CO and O$_2$ adsorption. A second result from the experimental protocol described in Scheme 2 is that it can be used to evaluate changes in the number of Au–CO binding sites. This is accomplished by simply comparing the area of the Au–CO adsorption peak ($\bar{v} = 2100$ cm^{-1}) before (step a) and after (step c) the CO oxidation reaction.

Table 5 shows that CO adsorption capacity is maintained even after extensive formation of carbonates on the catalyst. The only

Step	Gas Mix (time)	Purpose / Remarks
Pretreatment		Conditions shown in Table 1
N$_2$ flush	N$_2$ (1 hr)	Remove reactive gases (O$_2$, H$_2$)
CO adsorption (a)	1% CO/N$_2$ (10 min)	Determine Au-CO IR area (2100 cm^{-1})
CO oxidation (b)	1% CO/20% O$_2$/N$_2$ (10 min)	Monitor changes during CO Oxidation
CO adsorption (c)	1% CO/N$_2$ (10 min)	Evaluate any loss in sites during catalysis by changes in Au-CO band (2100 cm^{-1})
N$_2$ flush (d)	N$_2$ (30 min)	Remove weakly adsorbed species

Time on stream

Scheme 2. Sequential steps during in situ IR CO oxidation experiments. Reaction temperature, pressure, and gas flow were kept constant during the entire experiment (20 °C, ambient pressure, 100 mL/min).
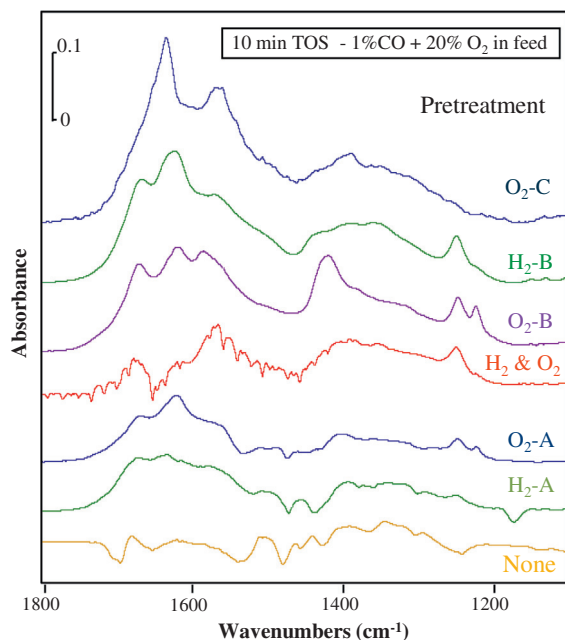
Fig. 6. Carbonates built-up on the catalysts after 10 min TOS CO oxidation at 20 °C (collected after step b of Scheme 2). Each spectrum was referenced to the catalyst immediately after pretreatment and cooling.

catalyst to show substantial loss of CO binding sites is the O_2-C treated catalyst, which has barely any activity. All the other catalysts show no statistically significant loss of CO binding sites – the Au–CO adsorption areas before and after CO oxidation catalysis are all within a very reasonable experimental error (<10%). Thus, the carbonates do not poison Au–CO binding sites and appear to reside essentially exclusively on the support. The changes in v_{max} must therefore be due to a change in the number of O_2 activation sites. It is also important to note that these experiments do not exclude the possibility that carbonates production merely correlates with the losses in catalytic activity, i.e., they correlate with some other, more subtle change to the catalyst but are not directly responsible for poisoning the catalyst.

4. Discussion

We performed this study to contribute to the understanding of how various pretreatments affect CO oxidation activity over Au/TiO_2, with the goals of trying to understand the relative importance of the pretreatment in affecting catalytic activity and identifying optimal activation protocols to maximize catalytic activity. We used a commercially available catalyst that had been pretreated by the manufacturer to ensure that particles were of appropriate size (2–4 nm) to yield active CO oxidation catalysts. This allows us to separate the effects of thermal treatments from those necessary for preparing active particles because the particle size does

not change as a function of the pretreatment [65–67]. Further, this catalyst has proven to be active and stable in spite of being stored over long periods of time, making it a useful benchmark material for comparing pretreatments and other catalysts.

This catalyst, which has been stored in a refrigerator in the dark for over a year, is clearly active and stable for CO oxidation with no additional thermal treatment (Fig. 1). Further, its activity has remained constant over nearly a year of testing. The activity of this untreated catalyst is comparable to or greater than most of the catalysts shown in Table 2. Many Au/TiO_2 catalysts can be found in the literature with much lower activities [11,46].

Fig. 1 clearly shows that catalytic activity is highly correlated with the "severity" of the thermal treatment. Although all the pretreatments showed reasonable initial activities, more forcing conditions – higher temperatures and longer times – produced catalysts with steady-state activities up to 10 times lower (treatments H_2-B and O_2-C) than the original untreated catalyst. This activity loss is not due to changing particle sizes (vide infra). It is possible that this activity loss may be partially due to localized heating during the first minutes of reaction. Although we cannot rule this out, diluting the catalyst (5 mg catalyst in 750 mg SiC) and running at low conversions (<10%), as was the case in these experiments, should minimize the influence of any differences in heating as the catalyst equilibrates with the reaction feed. No increase in the bed temperature was observed, and one pretreatment (H_2-B) showed a markedly slower approach to steady-state activity. If heating were the primary reason for the initial loss in activity, one would expect that the approach to steady state would be more consistent for all the pretreatments.
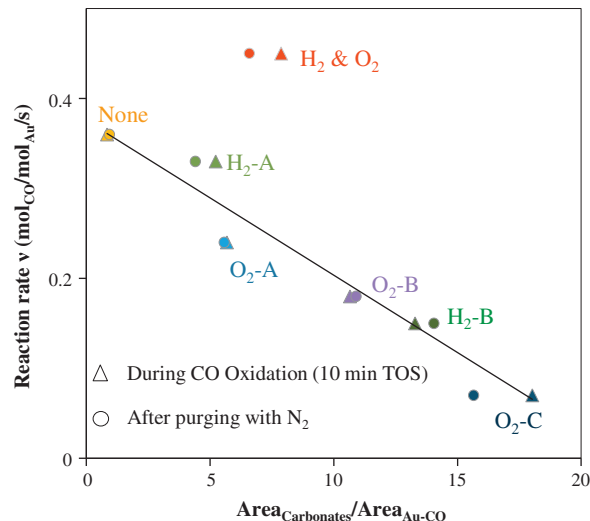

Fig. 7. CO oxidation catalytic activity vs. carbonates peak areas for different catalyst pretreatments. Carbonates IR region area was integrated in the range 1800–1200 cm^{-1} and normalized with respect to Au–CO area ($\bar{v} \sim 2100$ cm^{-1}).

Table 5
Integrated Au–CO peak areas before and after carbonates build up during CO oxidation.

Pretreatment	Initial $A_{(\bar{v}=2100)i}$	Post-reaction $A_{(\bar{v}=2100)f}$	Ratio $r = A_{(\bar{v}=2100)f}/A_{(\bar{v}=2100)i}$
None	4.61	4.36	0.95
O_2-A	4.74	4.70	0.99
H_2-A	4.55	4.89	1.07
H_2 and O_2	4.75	5.13	1.08
O_2-B	5.02	4.91	0.98
H_2-B	5.32	4.89	0.92
O_2-C	4.72	3.18	0.67

The subsequent studies were dedicated to understanding how changes to the catalyst during activation and CO oxidation might be responsible for the loss in activity. First and foremost, the loss of activity cannot be attributed to Au particle growth or sintering. We have previously performed TEM studies on this catalyst and found no change in particle size after treating this catalyst for 16 h at 300 °C, a longer time and higher temperature than all but one of the present pretreatments [49]. CO heat of adsorption metrics evaluated with the Temkin adsorption model are sensitive to particle size effects [57]; however, the heat of adsorption values for all the catalysts are essentially the same within very reasonable experimental errors (Fig. 2, Table 3), even for treatments that gave very low catalytic activities (treatments H₂-B and O₂-C). Further, our control experiments showed that the catalytic activity could be largely recovered by treating the catalyst with a short $H_2 + O_2$ treatment. This would not be possible if the deactivation resulted from (irreversible) Au nanoparticle growth. The lack of sintering is not surprising given that the catalyst was treated at 400 °C by the manufacturer; further treatment at lower temperatures should not substantially affect particle sizes.

4.1. Loss of active sites and carbonates buildup

Fig. 7 shows that the loss in the quasi-steady-state catalytic activity correlates with the buildup of surface carbonates. Closer inspection of Fig. 1 shows that all the catalysts have relatively high initial activities which decrease to a quasi-steady-state value, generally in about 10 min. This is qualitatively consistent with our observations during in situ IR experiments, which suggest that carbonates formation is generally complete after about 5 min on stream. Further, the M–M treatment of the kinetics data (Fig. 4, Table 4), which provides simultaneous measures of both the intrinsic catalytic activity of the active site and the number of active sites, indicates that the activity loss is primarily due to a loss in the relative number of active sites rather than changes to their intrinsic reactivity.

Supported Au catalysts are known to be prone to the formation of carbonate-like compounds [31,68–72]. Previous studies have correlated carbonates formation with catalytic activity, pretreatment conditions [23,73], presence of moisture in the gas [10,16], and reaction temperature [74]. Carbonates have also been shown to be decomposed in the presence of water [20], in the presence of H₂ [75], and during CO oxidation reaction at high temperatures [25,63].

The role that carbonate-like species play in catalytic activity has been under debate. Some researchers propose that bicarbonates [76–78], hydroxycarbonyls [71,79], and formates [11,79] are important CO oxidation intermediates. Others believe that carbonates are inert spectators to the catalysis [29,30,77,80]. Still others consider carbonates as catalyst poisons, acting according to one of two postulated poisoning mechanisms. The first attributes poisoning to carbonates formation on Au surfaces limiting CO adsorption on the catalysts [81]. The second stipulates that oxygen activation occurs at nanoparticle perimeter sites located at the metal–support interface. In this scheme, carbonates reside on the support, but block these perimeter sites, preventing oxygen activation [30].

All of the data in the present study show that carbonates formation correlates with lower catalytic activity due to a loss of active sites. Further, the observed carbonates are very stable on the catalyst, as their areas generally do not change after 10 min of flushing with nitrogen. Although we cannot rule out the possibility that unobserved transient carbonate-like species might be reaction intermediates, the observed carbonates do not decompose at rates comparable to the overall reaction rate and therefore cannot be intermediates in the reaction mechanism.

The activity loss correlates with the presence of surface carbonates; however, correlation is not equivalent to causation. The location of the carbonates therefore becomes a critical issue. The sequential IR experiments (Table 5) show that the CO adsorption capacity is unaffected even by extensive carbonates buildup. The carbonates must therefore reside on the support, since they do not poison the CO adsorption sites on Au. It should also be noted that in the case of extreme carbonates buildup (e.g., pretreatment H₂-B), there appears to be some loss of Au–CO binding sites, presumably due to carbonate migration from the support onto Au.

These results are therefore consistent with a poisoning model in which carbonates block Au perimeter sites; however, we do not have any direct evidence for how carbonates poison the reaction. Other possibilities should be considered, including that the surface carbonates indirectly poison the catalyst or that the presence of carbonates is reporting on some other more subtle change to the catalyst surface. For example, the FTIR spectroscopy experiments (Fig. 3) examined changes to the catalyst as a function of the pretreatment; it is clear that all of the pretreatments remove a substantial amount of water from the catalyst surface.

Several studies have shown that CO oxidation activity is sensitive to the water content in the feed and on the catalyst surface [16,18–20,68]. Iglesia and coworkers recently performed a kinetic isotope effect study, which suggested that water acts as a co-catalyst in the reaction [10]. The spectra in Fig. 3 are essentially the same in that each thermal treatment removes a qualitatively similar amount of water from the catalyst. There is no clear trend or correlation between water removal and catalytic activity, so it is unclear how catalyst water content might affect activity. Carbonates bind water very strongly [82], so carbonates production may simply sequester the remaining water on the catalyst, excluding it from the active site.

It is also widely accepted that CO oxidation activity over Au is closely tied to the presence of hydroxyl groups on the support [11,12]. Although the treatment temperatures that we have employed are not particularly strong, it is possible that the more forcing treatments induce some degree of surface dehydroxylation [83,84], possibly near the gold particles, and that the lower activity results from the removal of hydroxyl groups near the Au–TiO₂ perimeter sites. Unfortunately, any changes to the surface hydroxyl groups are masked by the large water peaks and, based on this data, it is impossible to say how much, if any, surface dehydroxylation occurs during the pretreatments.

It is also worth noting that the $H_2 + O_2$ treatment results in the most active of the catalyst pretreatments. This catalyst is flushed with nitrogen at the treatment temperature (as are all the others), and there are no obvious differences in the amount of water removed when this treatment is compared to the others (Fig. 3). However, the higher activity associated with this treatment, in spite of moderate carbonates formation, suggests that the water and/or hydroxyl groups may be more important for determining catalytic activity than are the surface carbonates. Precisely how this treatment works to activate the catalyst is unclear. It may prevent/mitigate poisoning by carbonates, leave a greater amount of active water on the surface, or affect surface hydroxylation near the Au particles. Hydrogen oxidation is well known to occur on Au [85–87] and is therefore likely to have the largest effect on hydroxylation of the support closest to the Au particles. Further studies are underway to evaluate these possibilities.

5. Conclusions

A commercial Au/TiO₂ catalyst was treated under different conditions prior to being used in CO oxidation. It was found that pretreatments with more severe conditions (longer times or higher

temperatures) produce a less active catalyst, and that the ranges of activities produced are similar to the range of different catalytic activities reported in the literature. The possibility that more severe thermal treatments cause nanoparticle sintering was evaluated with infrared spectroscopy of adsorbed CO combined with Temkin analysis. This methodology is sensitive to changes in particle size as well as the electronic configuration of the nanoparticles. The resulting thermodynamic values ΔH_o and $\delta \Delta H$ are consistent with no changes in particle size after different thermal treatments applied to the catalyst, consistent with our previous studies. Additional control experiments showed that catalytic activity after the harshest thermal treatments could be regenerated with a $H_2 + O_2$ treatment; thus, the activity loss could not be due to sintering. Infrared spectroscopy experiments showed that the thermal pretreatments remove water from the catalyst surface, but no correlation was found between the water loss and catalytic activity.

A Michaelis–Menten kinetic treatment indicates the reason behind catalyst deactivation is the loss of active sites; there was little change to the intrinsic reactivity of the active sites measured with this kinetic treatment. In other words, the remaining catalytically active sites have essentially the same inherent O_2 activation activity regardless of the pretreatment used. This activity loss coincided with the buildup of surface carbonates and led us to develop an in situ Fourier transform infrared (FTIR) spectroscopy experimental protocol for semi-quantitatively comparing the amount of surface carbonates produced on the catalyst. These experiments led to four primary conclusions: (1) more severe pretreatments lead to greater production of surface carbonates upon contact with the reaction feed, (2) the catalytic activity correlates well with the amount of carbonate-like species formed, (3) the observed carbonate-like species are strongly bound to the catalyst and are not intermediates in the reaction mechanism, and (4) the carbonates do not affect the CO adsorption capacity of the Au and therefore likely reside on the titania support.

All the experimental work done in the present research is consistent with a deactivation model in which higher levels of carbonates are related to an acute and fast deactivation of the catalysts. This idea contradicts several mechanistic models that propose that different carbonate-like species (carbonates, bicarbonates, hydroxicarbonates, carboxylates, etc.) are catalytic intermediates. However, it is not possible to establish that carbonate-like species are directly poisoning (or binding to) the Au nanoparticles.

Our experiments suggest that these species reside on the support, where it may be possible that they interfere with activity associated with perimeter sites on the Au particles. This interference could be due to carbonates reacting with surface hydroxyl groups on the support, thus limiting their availability to interact with Au perimeter sites, or possibly by sequestering surface H_2O and limiting its access to the Au nanoparticles. Both species (H_2O and support hydroxyls) are discussed in the literature as potentially being responsible for the high activity of Au/TiO_2 catalysts; however, this work does not shed light onto which may be more important at the catalytic active sites.

Acknowledgments

Appendix A. Supplementary material

Supplementary data associated with this article can be found, in the online version, at http://dx.doi.org/10.1016/j.jcat.2013.06.021.

References

[1] T. Ishida, M. Haruta, Angew. Chem. Int. Ed. 46 (2007) 7154–7156.
[2] M. Haruta, CATTECH 6 (2002) 102–115.
[3] H. Falsig, B. Hvolboek, I.S. Kristensen, T. Jiang, T. Bligaard, C.H. Christensen, J.K. Norskov, Angew. Chem. Int. Ed. 47 (2008) 4835–4839.
[4] D.W. Goodman, Catal. Lett. 99 (2005) 1–4.
[5] B.K. Min, C.M. Friend, Chem. Rev. 107 (2007) 2709–2724.
[6] S.H. Overbury, L. Ortiz-Soto, H. Zhu, B. Lee, M.D. Amiridis, S. Dai, Catal. Lett. 95 (2004) 99–106.
[7] S. Arrii, F. Morfin, A.J. Renouprez, J.L. Rousset, J. Am. Chem. Soc. 126 (2004) 1199–1205.
[8] M. Comotti, W.-C. Li, B. Spliethoff, F. Schueth, J. Am. Chem. Soc. 128 (2006) 917–924.
[9] M.S. Chen, D.W. Goodman, Science 306 (2004) 252–255.
[10] M. Ojeda, B.-Z. Zhan, E. Iglesia, J. Catal. 285 (2012) 92–102.
[11] M.C. Kung, R.J. Davis, H.H. Kung, J. Phys. Chem. C 111 (2007) 11767–11775.
[12] P. Ganesh, P.R.C. Kent, G.M. Veith, J. Phys. Chem. Lett. 2 (2011) 2918–2924.
[13] C.J. Karwacki, P. Ganesh, P.R.C. Kent, W.O. Gordon, G.W. Peterson, J.J. Niu, Y. Gogotsi, J. Mater. Chem. A 1 (2013) 6051–6062.
[14] K. Qian, W. Zhang, H. Sun, J. Fang, B. He, Y. Ma, Z. Jiang, S. Wei, J. Yang, W. Huang, J. Catal. 277 (2011) 95–103.
[15] K. Qian, J. Fang, W. Huang, B. He, Z. Jiang, Y. Ma, S. Wei, J. Mol. Catal. A: Chem. 320 (2010) 97–105.
[16] T. Yan, J. Gong, D.W. Flaherty, C.B. Mullins, J. Phys. Chem. C 115 (2011) 2057–2065.
[17] F. Gao, Y. Wang, D.W. Goodman, J. Phys. Chem. C 114 (2010) 4036–4043.
[18] T.A. De, H. Gies, W. Gruenert, Catal. Lett. 141 (2011) 1282–1287.
[19] M. Date, M. Haruta, J. Catal. 201 (2001) 221–224.
[20] M. Date, M. Okumura, S. Tsubota, M. Haruta, Angew. Chem. Int. Ed. 43 (2004) 2129–2132.
[21] M.M. Schubert, S. Hackenberg, V.A.C. van, M. Muhler, V. Plzak, R.J. Behm, J. Catal. 197 (2001) 113–122.
[22] T. Diemant, J. Bansmann, R.J. Behm, Vacuum 84 (2009) 193–196.
[23] N. Weiher, A.M. Beesley, N. Tsapatsaris, L. Delannoy, C. Louis, J.A. van Bokhoven, S.L.M. Schroeder, J. Am. Chem. Soc. 129 (2007) 2240–2241.
[24] M. Boronat, P. Concepcion, A. Corma, J. Phys. Chem. C 113 (2009) 16772–16784.
[25] D. Widmann, R.J. Behm, Angew. Chem. Int. Ed. 50 (2011) 10241–10245. S10241/10241–S10241/10246.
[26] M. Boronat, A. Corma, Dalton Trans. 39 (2010) 8538–8546.
[27] I.X. Green, W. Tang, M. Neurock, J.T. Yates Jr., Science (Washington, DC, US) 333 (2011) 736–739.
[28] M. Haruta, Faraday Discuss. 152 (2011) 11–32.
[29] M.C. Raphulu, J. McPherson, D.L.E. van, J.A. Anderson, M.S. Scurrell, Gold Bull. 43 (2010) 21–28.
[30] Y. Denkwitz, Z. Zhao, U. Hoermann, U. Kaiser, V. Plzak, R.J. Behm, J. Catal. 251 (2007) 363–373.
[31] P. Konova, A. Naydenov, C. Venkov, D. Mehandjiev, D. Andreeva, T. Tabakova, J. Mol. Catal. A: Chem. 213 (2004) 235–240.
[32] X. Bokhimi, R. Zanella, A. Morales, V. Maturano, C. Angeles-Chavez, J. Phys. Chem. C 115 (2011) 5856–5862.
[33] B. Schumacher, V. Plzak, J. Cai, R.J. Behm, Catal. Lett. 101 (2005) 215–224.
[34] J.H. Yang, J.D. Henao, M.C. Raphulu, Y. Wang, T. Caputo, A.J. Groszek, M.C. Kung, M.S. Scurrell, J.T. Miller, H.H. Kung, J. Phys. Chem. B 109 (2005) 10319–10326.
[35] H.H. Kim, S. Tsubota, M. Date, A. Ogata, S. Futamura, Appl. Catal. A 329 (2007) 93–98.
[36] G.C. Bond, C. Louis, D.T. Thompson, Catalysis by Gold, Imperial College Press, London, 2006.
[37] R. Zanella, S. Giorgio, C.R. Henry, C. Louis, J. Phys. Chem. B 106 (2002) 7634–7642.
[38] F. Boccuzzi, A. Chiorino, M. Manzoli, P. Lu, T. Akita, S. Ichikawa, M. Haruta, J. Catal. 202 (2001) 256–267.
[39] G.C. Bond, C. louis, D.T. Thompson, Influence of the Thermal Treatment on Gold Particle Size, Catalysis by Gold, Imperial College Press, London, 2006.
[40] J.D. Henao, T. Caputo, J.H. Yang, M.C. Kung, H.H. Kung, J. Phys. Chem. B 110 (2006) 8689–8700.
[41] J.T. Calla, R.J. Davis, J. Catal. 241 (2006) 407–416.
[42] S.H. Overbury, V. Schwartz, D.R. Mullins, W. Yan, S. Dai, J. Catal. 241 (2006) 56–65.
[43] J.T. Calla, M.T. Bore, A.K. Datye, R.J. Davis, J. Catal. 238 (2006) 458–467.
[44] G.R. Bamwenda, S. Tsubota, T. Nakamura, M. Haruta, Catal. Lett. 44 (1997) 83–87.
[45] T.V.W. Janssens, A. Carlsson, A. Puig-Molina, B.S. Clausen, J. Catal. 240 (2006) 108–113.
[46] V. Aguilar-Guerrero, B.C. Gates, Catal. Lett. 130 (2009) 108–120.
[47] P. Broqvist, L.M. Molina, H. Groenbeck, B. Hammer, J. Catal. 227 (2004) 217–226.

[48] B.D. Chandler, S. Kendell, H. Doan, R.J. Korkosz, L.C. Grabow, C.J. Pursell, ACS Catal. 2 (2012) 684–694.
[49] C.G. Long, J.D. Gilbertson, G. Vijayaraghavan, K.J. Stevenson, C.J. Pursell, B.D. Chandler, J. Am. Chem. Soc. 130 (2008) 10103–10115.
[50] C.J. Pursell, H. Hartshorn, T. Ward, B.D. Chandler, F. Boccuzzi, J. Phys. Chem. C 115 (2011) 23880–23892.
[51] H. Hartshorn, C.J. Pursell, B.D. Chandler, J. Phys. Chem. C 113 (2009) 10718–10725.
[52] R.J. Korkosz, J.D. Gilbertson, K.S. Prasifka, B.D. Chandler, Catal. Today 122 (2007) 370–377.
[53] A. Singh, B.D. Chandler, Langmuir 21 (2005) 10776–10782.
[54] H. Lang, S. Maldonado, K.J. Stevenson, B.D. Chandler, J. Am. Chem. Soc. 126 (2004) 12949–12956.
[55] H. Lang, R.A. May, B.L. Iversen, B.D. Chandler, J. Am. Chem. Soc. 125 (2003) 14832–14836.
[56] Samples are exposed to air and placed under vacuum for the CO adsorption experiments. Although we do not observe any effects from this transfer, we cannot rule out the possibility that the sample preparation may impact the measurements.
[57] C.J. Pursell, B.D. Chandler, M. Manzoli, F. Boccuzzi, J. Phys. Chem. C 116 (2012) 11117.
[58] A.D. Bykov, Y.S. Makushkin, O.N. Ulenikov, J. Mol. Spectrosc. 99 (1983) 221–227.
[59] B.D. Chandler, C.G. Long, J.D. Gilbertson, G. Vijayaraghavan, K.J. Stevenson, C.J. Pursell, J. Phys. Chem. C 114 (2010) 11498–11508.
[60] Our first paper deriving and employing the Michaelis–Menten treatment used K_I to describe O_2 reactivity. Based on various feedback, we have changed the name of the constant to K_R so that it is not confused with a constant designed to describe inhibition.
[61] M. Haruta, S. Tsubota, T. Kobayashi, H. Kageyama, M. Genet, B. Delmon, J. Catal. 144 (1993) 175.
[62] J.-D. Grunwaldt, A. Baiker, J. Phys. Chem. B 103 (1999) 1002–1012.
[63] Y. Denkwitz, B. Schumacher, G. Kucerova, R.J. Behm, J. Catal. 267 (2009) 78–88.
[64] The Au–CO area was calculated by subtracting the contribution of CO in the gas phase from the total CO stretching region (2000–2325 cm^{-1}). Using the formula $A(Au–CO) = A(2000–2325) − 2 * A(2225–2325)$, where $A(2225–2325)$ is the P-branch of the CO stretching vibration-rotation frequencies, we assume that the R- and P-branches are of equal intensity. This provides for a simple means of subtracting the absorbance due to gas phase CO.

[65] Z. Ma, C. Liang, S.H. Overbury, S. Dai, J. Catal. 252 (2007) 119–126.
[66] G. Walther, D.J. Mowbray, T. Jiang, G. Jones, S. Jensen, U.J. Quaade, S. Horch, J. Catal. 260 (2008) 86–92.
[67] C. Marsden, E. Taarning, D. Hansen, L. Johansen, S.K. Klitgaard, K. Egeblad, C.H. Christensen, Green Chem. 10 (2008) 168–170.
[68] F. Gao, T.E. Wood, D.W. Goodman, Catal. Lett. 134 (2010) 9–12.
[69] M.M. Schubert, V. Plzak, J. Garche, R.J. Behm, Catal. Lett. 76 (2001) 143–150.
[70] C.H. Kim, L.T. Thompson, J. Catal. 230 (2005) 66–74.
[71] C.K. Costello, M.C. Kung, H.S. Oh, Y. Wang, H.H. Kung, Appl. Catal. A 232 (2002) 159–168.
[72] F. Boccuzzi, A. Chiorino, S. Tsubota, M. Haruta, J. Phys. Chem. 100 (1996) 3625–3631.
[73] N. Hammer, K. Mathisen, T. Zscherpe, D. Chen, M. Ronning, Top. Catal. 54 (2011) 922–930.
[74] Y. Hao, R. Liu, X. Meng, H. Cheng, F. Zhao, J. Mol. Catal. A: Chem. 335 (2011) 183–188.
[75] H. Imai, M. Date, S. Tsubota, Catal. Lett. 124 (2008) 68–73.
[76] B. Schumacher, Y. Denkwitz, V. Plzak, M. Kinne, R.J. Behm, J. Catal. 224 (2004) 449–462.
[77] S.T. Daniells, A.R. Overweg, M. Makkee, J.A. Moulijn, J. Catal. 230 (2005) 52–65.
[78] L. Piccolo, H. Daly, A. Valcarcel, F.C. Meunier, Appl. Catal. B 86 (2009) 190–195.
[79] Y. Denkwitz, A. Karpenko, V. Plzak, R. Leppelt, B. Schumacher, R.J. Behm, J. Catal. 246 (2007) 74–90.
[80] M.A. Bollinger, M.A. Vannice, Appl. Catal. B 8 (1996) 417–443.
[81] B. Schumacher, V. Plzak, M. Kinne, R.J. Behm, Catal. Lett. 89 (2003) 109–114.
[82] E. Garand, T. Wende, D.J. Goebbert, R. Bergmann, G. Meijer, D.M. Neumark, K.R. Asmis, J. Am. Chem. Soc. 132 (2010) 849–856.
[83] R.L. Kurtz, R. Stockbauer, T.E. Madey, E. Roman, S.J.L. De, Surf. Sci. 218 (1989) 178–200.
[84] I.M. Brookes, C.A. Muryn, G. Thornton, Phys. Rev. Lett. 87 (2001). 266103/266101–266103/266104.
[85] I.X. Green, W. Tang, M. Neurock, J.T. Yates, Angew. Chem. Int. Ed. 50 (2011) 10186–10189.
[86] H. Dyrbeck, N. Hammer, M. Ronning, E.A. Blekkan, Top. Catal. 45 (2007) 21–24.
[87] D.A. Panayotov, S.P. Burrows, J.T. Yates, J.R. Morris, J. Phys. Chem. C 115 (2011) 22400–22408.